

Electroweak Precision Constraints on the Littlest Higgs Model with T Parity

Jay Hubisz, Patrick Meade, Andrew Noble, Maxim Perelstein*

*Institute for High Energy Phenomenology,
F.R. Newman Laboratory of Elementary Particle Physics,
Cornell University, Ithaca, NY 14853, USA*

hubisz@mail.lepp.cornell.edu, meade@mail.lepp.cornell.edu
an76@cornell.edu, maxim@mail.lepp.cornell.edu

Abstract

We compute the leading corrections to the properties of W and Z bosons induced at the one-loop level in the SU(5)/SO(5) Littlest Higgs model with T parity, and perform a global fit to precision electroweak data to determine the constraints on the model parameters. We find that a large part of the model parameter space is consistent with data. Values of the symmetry breaking scale f as low as 500 GeV are allowed, indicating that no significant fine tuning in the Higgs potential is required. We identify a region within the allowed parameter space in which the lightest T-odd particle, the partner of the hypercharge gauge boson, has the correct relic abundance to play the role of dark matter. In addition, we find that a consistent fit to data can be obtained for large values of the Higgs mass, up to 800 GeV, due to the possibility of a partial cancellation between the contributions to the T parameter from Higgs loops and new physics.

*Work supported by the National Science Foundation under grant PHY-0355005.

1 Introduction

The mechanism of electroweak symmetry breaking (EWSB) remains the most pressing puzzle in elementary particle physics. Experimentally, this question will be addressed at the Large Hadron Collider (LHC). Theoretically, several interesting possibilities have been proposed. In this article, we will concentrate on the “Little Higgs” proposal [1, 2]. In this approach, the Higgs emerges as a pseudo-Nambu-Goldstone boson, whose properties are constrained by global symmetries. These global symmetries are not exact, and their breaking allows the Higgs to participate in non-derivative (i.e. gauge and Yukawa) interactions. At the same time, there is enough global symmetry left to ensure that the Higgs mass term vanishes at tree level, and is only logarithmically sensitive to the unknown short distance (ultraviolet, or UV) physics at the one-loop level. The usual quadratic sensitivity of the Higgs mass parameter on the UV physics first appears at two loops, and the incalculable UV effects remain subleading as long as the cutoff of the theory (the scale at which it becomes strongly coupled) is at or below about 10 TeV. With this requirement, the Higgs mass terms are dominated by the one-loop contribution from the top loops, which has the appropriate sign to trigger the electroweak symmetry breaking, and produces the Higgs vacuum expectation value (vev) of the right order of magnitude. Thus, Little Higgs theories provide an attractive explanation of EWSB.

The originally proposed implementations of the Little Higgs approach suffered from severe constraints from precision electroweak measurements [3, 4, 5, 6], which could only be satisfied by finely tuning the model parameters. The most serious constraints resulted from the tree-level corrections to precision electroweak observables due to the exchanges of additional heavy gauge bosons present in the theories, as well as from the small but non-vanishing vev of an additional weak-triplet scalar field. Motivated by these constraints, several new implementations of the Little Higgs were proposed [7, 8, 9]. Particularly interesting is the approach of Refs. [10, 11, 12], which introduces a discrete symmetry, dubbed “T parity” in analogy to R parity in the minimal supersymmetric standard model (MSSM). T parity explicitly forbids any tree-level contribution from the heavy gauge bosons to the observables involving only standard model (SM) particles as external states. It also forbids the interactions that induced the triplet vev. As a result, in T parity symmetric Little Higgs models, corrections to precision electroweak observables are generated exclusively at loop level. This implies that the constraints are generically weaker than in the tree-level case, and fine tuning can be avoided [10, 11, 12].

The main goal of this paper is to investigate the electroweak precision constraints on the models with T parity in more detail. We will concentrate on the T parity symmetric version of the Littlest Higgs (LH) model, based on an $SU(5)/SO(5)$ global symmetry breaking pattern [11]. Some phenomenological aspects of this model have been analyzed in Ref. [13]. The model possesses an attractive dark matter candidate, the T-odd partner of the hypercharge gauge boson, which has the correct relic abundance in certain regions of the parameter space. It also leads to an interesting set of signatures at the LHC; in particular,

an excess of events with large missing transverse energy is expected. In this paper, we will compute the corrections to the properties of W/Z bosons induced by the new particles present in the LH model, and perform a global fit to precision electroweak observables. We will show that a consistent fit can be obtained in a large region of the model parameter space, so that no significant fine tuning is required. We will also demonstrate that the LH model allows for consistent fits with values of the Higgs mass as large as 800 GeV, far in excess of the upper bound obtained within the standard model. Finally, we will show that there exists a non-vanishing overlap between the region allowed by precision electroweak fits and the region where the LH model provides all of the observed dark matter.

The rest of the paper is organized as follows. After briefly reviewing the $SU(5)/SO(5)$ Littlest Higgs model with T parity in Section 2, we will present the calculation of the corrections to precision electroweak observables in Section 3. In Section 4, we present the constraints on the parameter space of the model resulting from a global fit to precision electroweak observables. Section 5 contains our conclusions. A discussion of some aspects of the LH model in the renormalizable R_ξ gauge, which we find useful in our calculations, is presented in the Appendix A.

2 The Model

In this section, we will review the LH model with T parity [11], emphasizing the features that will be important for the analysis of this paper.

2.1 Gauge-Scalar Sector

The Littlest Higgs model [1] embeds the electroweak sector of the standard model in an $SU(5)/SO(5)$ non-linear sigma model (nl σ m). A global $SU(5)$ symmetry is broken to $SO(5)$ by the vev of an $SU(5)$ symmetric tensor Σ of the form

$$\Sigma_0 = \begin{pmatrix} 0 & 0 & 0 & 1 & 0 \\ 0 & 0 & 0 & 0 & 1 \\ 0 & 0 & 1 & 0 & 0 \\ 1 & 0 & 0 & 0 & 0 \\ 0 & 1 & 0 & 0 & 0 \end{pmatrix}. \quad (2.1)$$

The low energy dynamics of the nl σ m is described in terms of the field

$$\Sigma = e^{2i\Pi/f} \Sigma_0, \quad (2.2)$$

where Π is the “pion matrix” containing the Goldstone degrees of freedom, and $f \sim 1$ TeV is the nl σ m symmetry breaking scale, or “pion decay constant”. An $[SU(2) \times U(1)]^2$ subgroup

of the global $SU(5)$ symmetry is gauged. The gauged generators have the form

$$\begin{aligned} Q_1^a &= \begin{pmatrix} \sigma^a/2 & 0 & 0 \\ 0 & 0 & 0 \\ 0 & 0 & 0 \end{pmatrix}, & Y_1 &= \text{diag}(3, 3, -2, -2, -2)/10, \\ Q_2^a &= \begin{pmatrix} 0 & 0 & 0 \\ 0 & 0 & 0 \\ 0 & 0 & -\sigma^{a*}/2 \end{pmatrix}, & Y_2 &= \text{diag}(2, 2, 2, -3, -3)/10. \end{aligned} \quad (2.3)$$

The kinetic term for the Σ field can be written as

$$\mathcal{L}_{\text{kin}} = \frac{f^2}{8} \text{Tr} D_\mu \Sigma (D^\mu \Sigma)^\dagger, \quad (2.4)$$

where

$$D_\mu \Sigma = \partial_\mu \Sigma - i \sum_j [g_j W_j^a (Q_j^a \Sigma + \Sigma Q_j^{aT}) + g'_j B_j (Y_j \Sigma + \Sigma Y_j)] , \quad (2.5)$$

with $j = 1, 2$. Here, B_j and W_j^a are the $U(1)_j$ and $SU(2)_j$ gauge fields, respectively, and g'_j and g_j are the corresponding coupling constants. The vev Σ_0 breaks the extended gauge group $[SU(2) \times U(1)]^2$ down to the diagonal subgroup, which is identified with the standard model electroweak group $SU(2)_L \times U(1)_Y$. The fourteen pions of the $SU(5)/SO(5)$ breaking decompose into representations of the electroweak gauge group as follows:

$$\mathbf{1}_0 \oplus \mathbf{3}_0 \oplus \mathbf{2}_{1/2} \oplus \mathbf{3}_{\pm 1}. \quad (2.6)$$

We will denote the fields in the above four representations as η , ω , H and ϕ , respectively. The field H has the appropriate quantum numbers to be identified with the SM Higgs; after EWSB, it can be decomposed as $H = (-i\pi^+, \frac{v+h+i\pi^0}{\sqrt{2}})^T$, where $v = 246$ GeV is the EWSB scale and h is the physical Higgs field. Explicitly, the pion matrix in terms of these fields has the form

$$\Pi = \begin{pmatrix} -\omega^0/2 - \eta/\sqrt{20} & -\omega^+/\sqrt{2} & -i\pi^+/\sqrt{2} & -i\phi^{++} & -i\frac{\phi^+}{\sqrt{2}} \\ -\omega^-/\sqrt{2} & \omega^0/2 - \eta/\sqrt{20} & \frac{v+h+i\pi^0}{2} & -i\frac{\phi^+}{\sqrt{2}} & \frac{-i\phi^0+\phi_P^0}{\sqrt{2}} \\ i\pi^-/\sqrt{2} & (v+h-i\pi^0)/2 & \sqrt{4/5}\eta & -i\pi^+/\sqrt{2} & (v+h+i\pi^0)/2 \\ i\phi^{--} & i\frac{\phi^-}{\sqrt{2}} & i\pi^-/\sqrt{2} & -\omega^0/2 - \eta/\sqrt{20} & -\omega^-/\sqrt{2} \\ i\frac{\phi^-}{\sqrt{2}} & \frac{i\phi^0+\phi_P^0}{\sqrt{2}} & \frac{v+h-i\pi^0}{2} & -\omega^+/\sqrt{2} & \omega^0/2 - \eta/\sqrt{20} \end{pmatrix}, \quad (2.7)$$

where the superscripts indicate the electric charge. The fields η and ω are eaten¹ when the extended gauge group is broken down to $SU(2)_L \times U(1)_Y$, whereas the π fields are

¹In the LH model with T parity, the fields η and ω mix with the field ϕ at order $(v/f)^2$, and it is a linear combination of these that is eaten. See Appendix A for details.

absorbed by the standard model W/Z bosons after EWSB. The fields h and ϕ remain in the spectrum. Including the EWSB effects, the vev of the Σ field has the form

$$\Sigma = \begin{pmatrix} 0 & 0 & 0 & 1 & 0 \\ 0 & -\frac{1}{2}(1 - c_v) & \frac{i}{\sqrt{2}}s_v & 0 & \frac{1}{2}(1 + c_v) \\ 0 & \frac{i}{\sqrt{2}}s_v & c_v & 0 & \frac{i}{\sqrt{2}}s_v \\ 1 & 0 & 0 & 0 & 0 \\ 0 & \frac{1}{2}(1 + c_v) & \frac{i}{\sqrt{2}}s_v & 0 & -\frac{1}{2}(1 - c_v) \end{pmatrix}, \quad (2.8)$$

where

$$s_v = \sin \frac{\sqrt{2}v}{f}, \quad c_v = \cos \frac{\sqrt{2}v}{f}. \quad (2.9)$$

These formulas will prove very useful for analyzing the spectrum of the model.

The gauge generators are embedded in the $SU(5)$ in such a way that any given generator commutes with an $SU(3)$ subgroup of the $SU(5)$. This implies that if one pair of gauge couplings (g_1, g'_1) or (g_2, g'_2) is set to zero, the Higgs field H would be an exact Goldstone boson and, therefore, exactly massless. Thus, any diagram renormalizing the Higgs mass vanishes unless it involves at least two of the gauge couplings. At one loop, all diagrams satisfying this property are only logarithmically divergent: the “collective” symmetry breaking mechanism protects the Higgs mass from quadratic divergences. The first quadratic divergence appears at two loop level.

The original Littlest Higgs model described above turned out to be significantly constrained by precision electroweak observables [3, 5, 6]. T parity, a discrete Z_2 symmetry, was introduced by Cheng and Low [10, 11] to avoid this difficulty, and it also provides a potential weak scale dark matter candidate. In the gauge sector, T parity is an automorphism of the gauge groups which exchanges the $[SU(2) \times U(1)]_1$ and $[SU(2) \times U(1)]_2$ gauge fields [11]. The Lagrangian in Eq. (2.4) is invariant under this transformation provided that $g_1 = g_2$ and $g'_1 = g'_2$. In this case, the gauge boson mass eigenstates (before EWSB) have the simple form, $W_{\pm} = (W_1 \pm W_2)/\sqrt{2}$, $B_{\pm} = (B_1 \pm B_2)/\sqrt{2}$, where W_+ and B_+ are the standard model gauge bosons and are T-even, whereas W_- and B_- are the additional, heavy, T-odd states. (Typically, B_- is the lightest T-odd state, and plays the role of dark matter [13].) After EWSB, the T-even neutral states W_+^3 and B_+ mix to produce the SM Z and the photon. Since they do not mix with the heavy T-odd states, the Weinberg angle is given by the SM relation, $\tan \theta_w = g'/g$, where $g = g_{1,2}/\sqrt{2}$ and $g' = g'_{1,2}/\sqrt{2}$ are the SM gauge couplings, and $\rho = 1$ at tree level. As will be shown below, all the SM fermions are also T-even, implying that the W_- and B_- states generate no corrections to precision electroweak observables at tree level.

The transformation properties of the gauge fields under T parity and the structure of the Lagrangian (2.4) imply that T parity acts on the pion matrix as follows:

$$T : \Pi \rightarrow -\Omega \Pi \Omega, \quad (2.10)$$

where $\Omega = \text{diag}(1, 1, -1, 1, 1)$. This transformation law ensures that the complex $SU(2)_L$ triplet ϕ is odd under T parity, while the Higgs doublet H is even. The trilinear coupling of the form $H^\dagger \phi H$ is therefore forbidden, and no triplet vev is generated. Eliminating this source of tree-level custodial $SU(2)$ violation further relaxes the precision electroweak constraints on the model.

2.2 Light Fermion Sector

In the original LH model, the fermion sector of the standard model remained unchanged with the exception of the third generation of quarks, where the top Yukawa coupling had to be modified to avoid the large quadratically divergent contribution to the Higgs mass from top loops. In the model with T parity, however, the standard model fermion doublet spectrum needs to be doubled to avoid compositeness constraints [11]. For each lepton/quark doublet, two fermion doublets $\psi_1 \in (\mathbf{2}, \mathbf{1})$ and $\psi_2 \in (\mathbf{1}, \mathbf{2})$ are introduced. (The quantum numbers refer to representations under the $SU(2)_1 \times SU(2)_2$ gauge symmetry.) These can be embedded in incomplete representations Ψ_1, Ψ_2 of the global $SU(5)$ symmetry. An additional set of fermions forming an $SO(5)$ multiplet Ψ^c , transforming nonlinearly under the full $SU(5)$, is introduced to give mass to the extra fermions; the field content can be expressed as follows:

$$\Psi_1 = \begin{pmatrix} \psi_1 \\ 0 \\ 0 \end{pmatrix}, \quad \Psi_2 = \begin{pmatrix} 0 \\ 0 \\ \psi_2 \end{pmatrix}, \quad \Psi^c = \begin{pmatrix} \psi^c \\ \chi^c \\ \tilde{\psi}^c \end{pmatrix}. \quad (2.11)$$

These fields transform under the $SU(5)$ as follows:

$$\Psi_1 \rightarrow V^* \Psi_1, \quad \Psi_2 \rightarrow V \Psi_2, \quad \Psi^c \rightarrow U \Psi^c, \quad (2.12)$$

where U is the nonlinear transformation matrix defined in Refs. [11, 12, 13]. The action of T parity on the multiplets takes

$$\Psi_1 \leftrightarrow -\Sigma_0 \Psi_2, \quad \Psi^c \rightarrow -\Psi^c. \quad (2.13)$$

These assignments allow a term in the Lagrangian of the form

$$\kappa f (\bar{\Psi}_2 \xi \Psi^c + \bar{\Psi}_1 \Sigma_0 \Omega \xi^\dagger \Omega \Psi^c), \quad (2.14)$$

where $\xi = \exp(i\Pi/f)$. This term gives a Dirac mass $M_- = \sqrt{2}\kappa f$ to the T-odd linear combination of ψ_1 and ψ_2 , $\psi_- = (\psi_1 + \psi_2)/\sqrt{2}$, together with $\tilde{\psi}^c$; the T-even linear combination, $\psi_+ = (\psi_1 - \psi_2)/\sqrt{2}$, remains massless and is identified with the standard model lepton or quark doublet. To give Dirac masses to the remaining T-odd states χ^c and ψ^c , additional fermions with opposite gauge quantum numbers can be introduced [11, 12, 13].

To complete the discussion of the fermion sector, we introduce the usual SM set of the $SU(2)_L$ -singlet leptons and quarks, which are T-even and can participate in the SM Yukawa

interactions with ψ_+ . The Yukawa interactions induce a one-loop quadratic divergence in the Higgs mass; however, the effect is numerically small except for the third generation of quarks. The Yukawa couplings of the third generation must be modified to incorporate the collective symmetry breaking pattern; this is discussed in the next subsection.

2.3 Top Sector

In order to avoid large one-loop quadratic divergences from the top sector, the Ψ_1 and Ψ_2 multiplets for the third generation must be completed to representations of the $SU(3)_1$ (“upper-left corner”) and $SU(3)_2$ (“lower-right corner”) subgroups of $SU(5)$. These multiplets are

$$\mathcal{Q}_1 = \begin{pmatrix} q_1 \\ U_{L1} \\ 0 \end{pmatrix}, \quad \mathcal{Q}_2 = \begin{pmatrix} 0 \\ U_{L2} \\ q_2 \end{pmatrix}; \quad (2.15)$$

they obey the same transformation laws under T parity and the $SU(5)$ symmetry as do Ψ_1 and Ψ_2 , see Eqs. (2.12) and (2.13). The quark doublets are embedded such that

$$q_i = -\sigma_2 \begin{pmatrix} u_{Li} \\ b_{Li} \end{pmatrix}. \quad (2.16)$$

In addition to the SM right-handed top quark field u_R , which is assumed to be T-even, the model contains two $SU(2)_L$ -singlet fermions U_{R1} and U_{R2} of hypercharge 2/3, which transform under T parity as

$$U_{R1} \leftrightarrow -U_{R2}. \quad (2.17)$$

The top Yukawa couplings arise from the Lagrangian of the form

$$\begin{aligned} \mathcal{L}_t = & \frac{1}{2\sqrt{2}} \lambda_1 f \epsilon_{ijk} \epsilon_{xy} [(\bar{\mathcal{Q}}_1)_i \Sigma_{jx} \Sigma_{ky} - (\bar{\mathcal{Q}}_2 \Sigma_0)_i \tilde{\Sigma}_{jx} \tilde{\Sigma}_{ky}] u_R \\ & + \lambda_2 f (\bar{U}_{L1} U_{R1} + \bar{U}_{L2} U_{R2}) + \text{h.c.} \end{aligned} \quad (2.18)$$

where $\tilde{\Sigma} = \Sigma_0 \Omega \Sigma^\dagger \Omega \Sigma_0$ is the image of the Σ field under T parity, see Eq. (2.10), and the indices i, j, k run from 1 to 3 whereas $x, y = 4, 5$. The T parity eigenstates are given by

$$q_\pm = \frac{1}{\sqrt{2}}(q_1 \mp q_2), \quad U_{L\pm} = \frac{1}{\sqrt{2}}(U_{L1} \mp U_{L2}), \quad U_{R\pm} = \frac{1}{\sqrt{2}}(U_{R1} \mp U_{R2}). \quad (2.19)$$

In terms of these eigenstates, Eq. (2.18) has the form

$$\mathcal{L}_m^T = \lambda_1 f \left[\frac{1}{2}(1 + c_v) \bar{U}_{L+} + \frac{s_v}{\sqrt{2}} \bar{u}_{L+} \right] u_R + \lambda_2 f (\bar{U}_{L+} U_{R+} + \bar{U}_{L-} U_{R-}) + \text{h.c.} \quad (2.20)$$

where we have used Eq. (2.8). The T-odd states U_{L-} and U_{R-} combine to form a Dirac fermion T_- , with mass $m_{T_-} = \lambda_2 f$. The remaining T-odd states q_- receive a Dirac mass

from the interaction in Eq. (2.14), and are assumed to be decoupled. The mass terms for the T-even states are diagonalized by defining

$$\begin{aligned} t_L &= \cos \beta u_{L+} - \sin \beta U_{L+}, & T_{L+} &= \sin \beta u_{L+} + \cos \beta U_{L+}, \\ t_R &= \cos \alpha u_R - \sin \alpha U_{R+}, & T_{R+} &= \sin \alpha u_R + \cos \alpha U_{R+}, \end{aligned} \quad (2.21)$$

where t is identified with the SM top and T_+ is its T-even heavy partner. The mixing angles are given by

$$\begin{aligned} \alpha &= \frac{1}{2} \tan^{-1} \frac{4\lambda_1\lambda_2(1+c_v)}{4\lambda_2^2 - \lambda_1^2(2s_v^2 + (1+c_v)^2)}, \\ \beta &= \frac{1}{2} \tan^{-1} \frac{2\sqrt{2}\lambda_1^2 s_v(1+c_v)}{4\lambda_2^2 + (1+c_v)^2\lambda_1^2 - 2\lambda_1^2 s_v}. \end{aligned} \quad (2.22)$$

To leading order in the v/f expansion,

$$\sin \alpha = \frac{\lambda_1}{\sqrt{\lambda_1^2 + \lambda_2^2}}, \quad \sin \beta = \frac{\lambda_1^2}{\lambda_1^2 + \lambda_2^2} \frac{v}{f}. \quad (2.23)$$

The masses of the two T-even Dirac fermions are given by

$$m_{t,T_+}^2 = f^2 \Delta \left(1 \pm \sqrt{1 - \frac{\lambda_1^2 \lambda_2^2 s_v^2}{2\Delta^2}} \right), \quad (2.24)$$

where

$$\Delta = \frac{1}{2} \left(\lambda_2^2 + \frac{\lambda_1^2}{2}(s_v^2 + \frac{1}{2}(1+c_v)^2) \right). \quad (2.25)$$

To leading order in v/f ,

$$m_t = \frac{\lambda_1 \lambda_2 v}{\sqrt{\lambda_1^2 + \lambda_2^2}}, \quad m_{T_+} = \sqrt{\lambda_1^2 + \lambda_2^2} f. \quad (2.26)$$

It is interesting to note that the T-odd states do not participate in the cancellation of quadratic divergences in the top sector: the cancellation only involves loops of t and T_+ , and the details are identical to the LH model without T parity [5].

Using the above equations, it is straightforward to obtain the Feynman rules for the top sector of the LH model; we list the rules relevant for the calculations in this paper in Table 1.

3 Corrections to Precision Electroweak Observables

The introduction of T parity automatically eliminates the tree level electroweak precision constraints that plagued the original Littlest Higgs model: since the external states in all

Particles	Vertices	Particles	Vertices
$Z\bar{t}t$	$\frac{ec_\beta^2}{s_w c_w} \left(T^3 - \frac{2}{3} \frac{s_w^2}{c_\beta^2} \right)$	$Z\bar{T}_-T_-$	$-\frac{2}{3} \frac{e s_w}{c_w}$
ZT_+T_+	$\frac{e}{s_w c_w} \left(s_\beta^2 T^3 - \frac{2}{3} s_w^2 \right)$	$Wb_L t_L$	$\frac{ec_\beta}{s_w}$
$Z\bar{t}T_+$	$-\frac{es_\beta c_\beta}{s_w c_w} T^3$	$Wb_L T_{+L}$	$-\frac{es_\beta}{s_w}$

Table 1: Feynman rules relevant for the analysis of the top sector of the LH model with T parity in this paper. We have defined $s_\beta \equiv \sin \beta$, $c_\beta \equiv \cos \beta$; s_w, c_w denote the sine and cosine of the weak mixing angle; and $T^3 = Q_1^3 + Q_2^3$ is the diagonal generator of $SU(2)_L$.

experimentally tested processes are T-even, no T-odd state can contribute to such processes at tree level. The only non-SM T-even state in our model, the heavy top T_+ , can only contribute at tree level to observables involving the SM top quark², such as its couplings to W and Z bosons [14]. At present, however, these couplings have not been measured experimentally, so no constraints arise at the tree level. At one-loop level, however, precision electroweak observables receive contributions from the T_+ as well as the T-odd particles. It is these contributions that determine the allowed parameter space of the Littlest Higgs model with T parity. We will evaluate the leading corrections in this section, and use them to perform a global fit to precision electroweak observables in Section 4.

In the SM, one-loop contributions to precision electroweak observables from the top sector, enhanced by powers of the top Yukawa coupling λ_t , dominate over contributions from the gauge and scalar sectors. We expect that the same hierarchy of effects will hold in the Littlest Higgs model, and our main focus will be on analyzing the effects of the top sector. However, we will also include the custodial-symmetry violating contributions from the gauge sector and the T-odd partners of light fermions, which become important in certain regions of the parameter space. In addition, we will show explicitly that the contributions from the complex scalar triplet, which were shown to be potentially important in the original LH model [6], completely decouple in the T parity symmetric case due to the absence of the triplet vev.

Before proceeding with the calculations, let us make the following comment. The nlsM underlying the LH model is a non-renormalizable effective theory, valid up to a cutoff scale $\Lambda \sim 4\pi f$. Every operator consistent with the symmetries of the low-energy theory will be generated at the cutoff scale Λ , and will contribute to the precision electroweak observables. However, we do not include such operators in the fit. (The only exception we make is to include the leading operator contributing to the T parameter, Eq. (3.33), since this parameter plays the most important role in constraining the model.) This is justified by the following considerations. First, while the contribution of the TeV-scale states that we will compute and the operator contributions that we will ignore are naively of the same order, $v^2/(16\pi^2 f^2) \sim v^2/\Lambda^2$, the former are logarithmically enhanced by a factor of $\log(f^2/v^2) \sim \log(\Lambda^2/f^2) \sim \log(4\pi)^2 \sim 5$. Second, while a cancellation between

²Tree-level contributions of T_+ to other observables are suppressed by small off-diagonal CKM matrix elements.

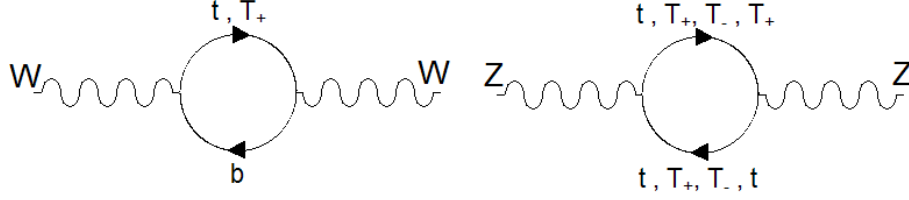


Figure 1: The one-loop diagrams contributing to the oblique corrections from the top sector of the LH model with T parity.

the corrections computed below and the operator contribution is in principle possible if the UV physics produces an operator with a large coefficient, any significant change in the fits due to such a cancellation would represent a fine-tuning between the effects generated at two different energy scales, f and Λ .

3.1 Oblique Corrections

The largest corrections to precision electroweak observables in the LH model are induced by the one-loop diagrams involving the T-even T_+ quark shown in Fig. 1. These oblique corrections can be described in terms of the Peskin-Takeuchi S , T , and U parameters [15]. The calculation of these parameters is straightforward if somewhat tedious; the result is

$$\begin{aligned}
S &= \frac{s_\beta^2}{2\pi} \left[\left(\frac{1}{3} - c_\beta^2 \right) \log x_t + \frac{(1+x_t)^2}{(1-x_t)^2} + \frac{2x_t^2(3-x_t) \log x_t}{(1-x_t)^3} - \frac{8}{3} \right], \\
T &= \frac{3}{16\pi} \frac{s_\beta^2}{s_w^2 c_w^2} \frac{m_t^2}{m_Z^2} \left[\frac{s_\beta^2}{x_t} - 1 - c_\beta^2 - \frac{2c_\beta^2}{1-x_t} \log x_t \right], \\
U &= -\frac{s_\beta^2}{2\pi} \left[s_\beta^2 \log x_t + \frac{(1+x_t)^2}{(1-x_t)^2} + \frac{2x_t^2(3-x_t) \log x_t}{(1-x_t)^3} - \frac{8}{3} \right], \tag{3.27}
\end{aligned}$$

where $x_t = m_t^2/m_{T_+}^2$, s_β is the sine of the left-handed t - T_+ mixing angle given in Eq. (2.22), and s_w is the sine of the Weinberg angle. In the limit when $x_t \ll 1$, these formulas simplify considerably and we obtain

$$\begin{aligned}
S &= \frac{1}{3\pi} \left(\frac{\lambda_1}{\lambda_2} \right)^2 \frac{m_t^2}{m_{T_+}^2} \left[-\frac{5}{2} + \log \frac{m_{T_+}^2}{m_t^2} \right], \\
T &= \frac{3}{8\pi} \frac{1}{s_w^2 c_w^2} \left(\frac{\lambda_1}{\lambda_2} \right)^2 \frac{m_t^4}{m_{T_+}^2 m_Z^2} \left[\log \frac{m_{T_+}^2}{m_t^2} - 1 + \frac{1}{2} \left(\frac{\lambda_1}{\lambda_2} \right)^2 \right], \\
U &= \frac{5}{6\pi} \left(\frac{\lambda_1}{\lambda_2} \right)^2 \frac{m_t^2}{m_{T_+}^2}. \tag{3.28}
\end{aligned}$$

The leading-order result for the T parameter is in agreement with the previous analyses of LH models with and without T parity [3, 6, 11].

In contrast to T_+ , the T -odd top partner T_- does not contribute to S, T or U since it is an $SU(2)_L$ singlet which does not mix with the SM top. However, T_- loops do affect precision electroweak observables at the level of $(m_Z/m_{T_-})^2$ corrections which are not captured by the formalism of Peskin and Takeuchi. The corrections to the two most precisely measured observables, $s_W \equiv (1 - m_W^2/m_Z^2)^{1/2}$ and s_* (the value of the weak mixing angle implied from Z decay asymmetries), are given by

$$s_*^2 - s_0^2 = -\frac{2\alpha}{45\pi} \frac{c_w^2 s_w^2}{c_w^2 - s_w^2} \frac{m_Z^2}{m_{T_-}^2}, \quad s_W^2 - s_*^2 = 0, \quad (3.29)$$

where s_0 is the reference value of the weak mixing angle inferred from

$$s_0^2(1 - s_0^2) = \frac{\pi\alpha}{\sqrt{2}G_F m_Z^2}. \quad (3.30)$$

These corrections are very small, and we do not include them in the global fit performed in Section 4.

It is clear from Eqs. (3.28) that the T parameter induced by the T_+ loops is about 20 times larger than the S and the U for the same model parameters, and therefore the constraints on the model are largely driven by the T parameter. This parameter also receives a contribution from the gauge sector of the model. While in general subdominant, this correction becomes important when the $t - T_+$ mixing is suppressed (namely when the ratio λ_1/λ_2 is small), and we will include it in the fit. This contribution arises from the custodial $SU(2)$ -violating tree level mass splitting of the T -odd heavy W_H^3 and W_H^\pm gauge bosons. Neglecting effects of order g'^2 , the mass splitting is given by

$$\Delta M^2 \equiv M^2(W_H^3) - M^2(W_H^\pm) = \frac{g^2 f^2}{4} (1 - c_v)^2 \approx \frac{1}{8} g^2 \frac{v^4}{f^2}. \quad (3.31)$$

At one loop, this effect induces a contribution to the T parameter [11]:³

$$T_{W_H} = -\frac{9}{16\pi c_w^2 s_w^2 M_Z^2} \Delta M^2 \log \frac{\Lambda^2}{M^2(W_H)}. \quad (3.32)$$

Note that the result is divergent, and depends on the UV cutoff of the theory Λ . This should not be surprising since the theory we're dealing with is non-renormalizable: indeed, the mass splitting in Eq. (3.31) comes from a dimension-6 operator of the form $W^\mu W_\mu (H^\dagger H)^2$, which appears when the Σ fields in Eq. (2.4) are expanded to order Π^4 . The UV divergence signals the presence of a “counterterm” operator of the form [11]

$$\mathcal{L}_c = \delta_c \frac{g^2}{16\pi^2} f^2 \sum_{i,a} \text{Tr} [(Q_i^a D_\mu \Sigma)(Q_i^a D^\mu \Sigma)^*], \quad (3.33)$$

³We find that the calculation of this contribution simplifies considerably in the Landau gauge, $\xi = 0$.

where δ_c is an order-one coefficient whose exact value depends on the details of the UV physics. (The normalization of Eq. (3.33) is fixed by naive dimensional analysis [16].) Including the counterterm, the full contribution of the gauge sector to the T parameter has the form

$$T = -\frac{1}{4\pi s_w^2} \frac{v^2}{f^2} \left(\delta_c + \frac{9}{8} \log \frac{\Lambda^2}{M^2(W_H)} \right) = -\frac{1}{4\pi s_w^2} \frac{v^2}{f^2} \left(\delta_c + \frac{9}{4} \log \frac{4\pi}{g} \right). \quad (3.34)$$

where we have assumed $\Lambda = 4\pi f$ and used $M(W_H) = gf$. As expected, this contribution is parametrically subdominant to the correction from the top sector, Eq. (3.28), in the limit $m_t \gg m_Z$. Furthermore, in agreement with the discussion at the beginning of this section, the effect of the operator (3.33) induced at the cutoff scale is subdominant, by a factor of $1/\log(\Lambda^2/M^2(W_H)) \sim 0.2$, compared to the calculable contribution in Eq. (3.32).

In Section 4, we will also be interested in the effects of varying the Higgs mass. To leading order, the Higgs contribution to the oblique parameters is given by [15]

$$\begin{aligned} S &= \frac{1}{12\pi} \log \frac{m_h^2}{m_{h,\text{ref}}^2}, \\ T &= -\frac{3}{16\pi c_w^2} \log \frac{m_h^2}{m_{h,\text{ref}}^2}, \\ U &= 0, \end{aligned} \quad (3.35)$$

where $m_{h,\text{ref}} \ll m_h$ is the “reference” value of the Higgs mass used to obtain the SM predictions for precision electroweak observables⁴. Interestingly, the negative contribution to the T parameter from a heavy Higgs can be partially cancelled by the positive contribution from the T_+ . As we will show below, this cancellation allows for a consistent fit to precision electroweak observables with the Higgs mass well above the upper bound obtained in the SM [17].

Finally, the LH model contains an additional T-odd $SU(2)_L$ -triplet scalar field ϕ , with the mass

$$m_\phi^2 \approx \frac{2m_h^2 f^2}{v^2} \sim (1 \text{ TeV})^2. \quad (3.36)$$

After EWSB, a mass splitting of order v^2/f between various components of the triplet is generated, for example, by operators of the form $H^\dagger \phi \phi^\dagger H$. Neglecting this mass splitting, the triplet contributions to S , T and U parameters vanish; keeping the terms of order $(m_Z/m_\phi)^2$, its contributions to s_* and s_W are given by

$$s_*^2 - s_0^2 = -\frac{\alpha}{24\pi} \frac{s_w^2 c_w^2}{c_w^2 - s_w^2} \frac{m_Z^2}{m_\phi^2}, \quad s_W^2 - s_*^2 = \frac{\alpha}{60\pi} \frac{m_W^2}{m_\phi^2}. \quad (3.37)$$

⁴It should be kept in mind that in the LH model, the Higgs couplings to the W/Z bosons will receive corrections of order v/f , which have been neglected in Eq. (3.35). This will not affect any of the conclusions of our analysis in Section 4.

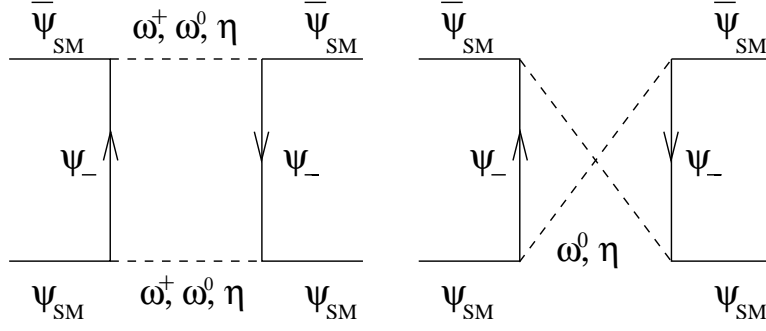


Figure 2: The box diagrams which provide the leading contribution to the four-fermion operators in the limit $\kappa \gg g$.

If the mass splitting is taken into account, non-zero contributions to the Peskin-Takeuchi parameters are induced; however, these effects are of order $\Delta m_\phi^2/m_\phi^2 \sim v^4/m_\phi^4$, and are thus subleading to the corrections given in Eq. (3.37). We conclude that the effects of the triplet ϕ on the precision electroweak observables in the LH model with T parity decouple with growing m_ϕ , and are negligible for m_ϕ in its natural range, around 1 TeV. We will not include these effects in the global fit of Section 4.

3.2 Effects of the T-Odd Partners of Light Fermions

To implement T parity in the fermion sector of the LH model, it is necessary to introduce a T-odd fermion partner for each lepton/quark doublet of the SM (see Section 2.2). These particles are vector-like, and their effects on precision electroweak observables must decouple in the limit when their mass is taken to infinity. However, box diagrams involving the exchanges of Goldstone bosons ω and η , see Fig. 2, generate four-fermion operators whose coefficients *increase* if the mass of the T-odd fermions is increased while f is kept fixed⁵. This non-decoupling is easy to understand qualitatively: to increase the mass of the T-odd fermions, it is necessary to increase the Yukawa coupling κ in Eq. (2.14), which in turn makes the four interaction vertices in the box diagrams stronger. Assuming that the couplings κ are flavor-diagonal and flavor-independent, the generated operators have the form

$$\mathcal{O}_{4-f} = -\frac{\kappa^2}{128\pi^2 f^2} \bar{\psi}_L \gamma^\mu \psi_L \bar{\psi}'_L \gamma_\mu \psi'_L, \quad (3.38)$$

where ψ and ψ' are (distinct) SM fermions, and we ignore the corrections of order g/κ . The experimental bounds on four-fermi interactions involving SM fields provide an *upper* bound on the T-odd fermion masses; the strongest constraint comes from the *eedd* operator, whose coefficient is required to be smaller than $2\pi/(26.4 \text{ TeV})^2$ [17]. This yields

$$M_{\text{TeV}} \lesssim 4.8 f_{\text{TeV}}^2, \quad (3.39)$$

⁵We are grateful to Thomas Gregoire for bringing this point to our attention.

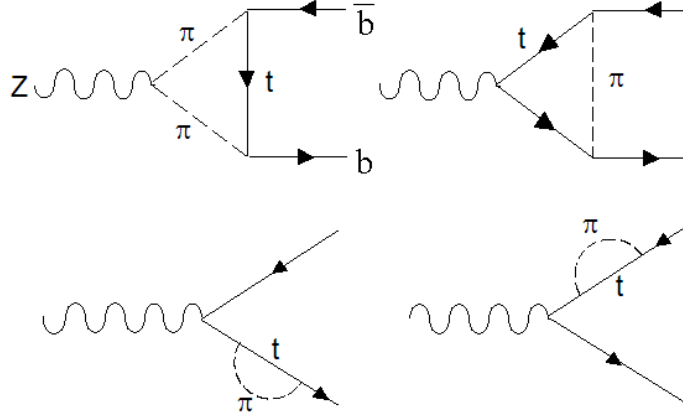


Figure 3: The dominant standard model diagrams which contribute to the $Zb\bar{b}$ vertex renormalization at one-loop in the R_ξ gauge.

where M_{TeV} and f_{TeV} are the values of the T-odd fermion masses and the symmetry breaking scale, respectively, in TeV. In addition, a lower bound on the masses of the T-odd fermions can be obtained from non-observation of these particles at the Tevatron; in analogy with squarks of the MSSM, we expect the bound to be in the neighborhood of 250–300 GeV.

The contribution of each T-odd doublet to the T parameter is given by

$$T_{\text{T-odd}} = -\frac{\kappa^2}{192\pi^2\alpha} \left(\frac{v}{f}\right)^2, \quad (3.40)$$

where we omit terms of order $(v/f)^4$ and higher. Note that, for a fixed value of f , this contribution *increases* with increasing T-odd fermion mass; Eq. (3.39) implies that

$$|T_{\text{T-odd}}| \lesssim 0.05, \quad (3.41)$$

independent of f . (Note that this bound relies on the assumption that the κ couplings are flavor-independent.) Nevertheless, the T-odd fermions can have a noticeable effect on the precision electroweak fits due to a large number (twelve) of doublets in the SM; this will be illustrated in the next section.

3.3 $Z \rightarrow b\bar{b}$ Vertex Renormalization

In the SM, the largest non-oblique correction is the renormalization of the $Zb\bar{b}$ vertex by top quark loops. This effect is non-decoupling in the sense that it is proportional to the square of the top mass. This non-decoupling is most easily seen if the calculation is performed in the 't Hooft-Feynman gauge [18]. In this gauge, the non-decoupling part of the vertex correction comes purely from the diagrams involving the exchange of a Goldstone boson π^\pm , since its couplings to the top and bottom quarks are enhanced by the top Yukawa λ_t . These

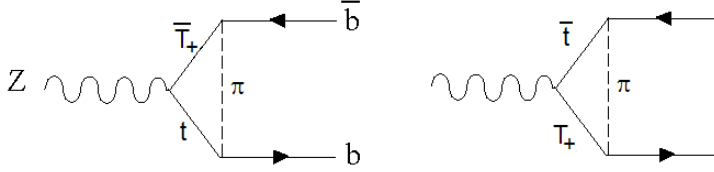


Figure 4: The additional “mixing” diagrams contributing to the $Zb\bar{b}$ vertex renormalization at one loop in the LH model with T parity.

diagrams are shown in Fig. 3. The diagrams involving the exchange of the gauge bosons are subdominant in the large- m_t limit, and neglecting their contribution only induces an error of order $(m_Z/m_t)^2 \sim 25\%$ in the vertex correction calculation.

We have calculated the one-loop correction to the $Zb\bar{b}$ vertex in the LH model with T parity. We used the ’t Hooft-Feynman gauge (for a brief discussion of the R_ξ gauges in the LH model, see Appendix A). As in the SM case, the diagrams involving π^\pm exchanges dominate in the large- m_t limit, and we neglected all other contributions. (While a more precise calculation could be done, the effort would not be justified as the $Zb\bar{b}$ correction turns out to have only a small effect on precision electroweak fits.) These diagrams are of three kinds. First, the same diagrams as in the SM appear, but with the top coupling to the Z modified according to Table 1. Second, all the diagrams in Fig. 3 also appear with the top replaced by the T-even heavy top partner T_+ . Third, the “mixing” diagrams shown in Fig. 4 appear as a result of the mixing between t and T_+ . These diagrams can be easily calculated using the couplings given in Table 1 and in Eq. (A.54) of Appendix A. To leading order in the limit $m_{T_+} \gg m_t \gg m_W$, the result is

$$\delta g_L^{b\bar{b}} = \frac{g}{c_w} \frac{\alpha}{8\pi s_w^2} \frac{m_t^4}{m_W^2 m_{T_+}^2} \frac{\lambda_1^2}{\lambda_2^2} \log \frac{m_{T_+}^2}{m_t^2}, \quad (3.42)$$

where $\delta g_L^{b\bar{b}}$ is the correction received by the $Zb_L\bar{b}_L$ vertex in the LH model *in addition* to the usual SM one-loop correction. It is interesting to note that this leading order contribution comes entirely from the mixing diagrams in Fig. 4. The correction to the $Zb_R\bar{b}_R$ vertex is negligible since it is not enhanced by the top Yukawa coupling. Note also that the correction in Eq. (3.42) does not have the correct sign to alleviate the well-known deviation of the measured value of the forward-backward asymmetry in $Z \rightarrow b\bar{b}$ decays from the SM prediction inferred from the other precision electroweak observables [19].

A calculation of $Zb\bar{b}$ in a general theory containing an extra heavy quark that mixes with t has been carried out in Ref. [20]. Accounting for the fact that U_+ is a vector isosinglet and including the appropriate mixing specific to the LH model, Eq. (3.42) agrees with the results of this analysis in the limit $m_{T_+} \gg m_t \gg m_W$. The results of Ref. [20] are more general, valid for arbitrary values of m_{T_+} and m_t . However, we find that using these expressions instead of Eq. (3.42) does not lead to noticeable changes in the global fits performed in Section 4.

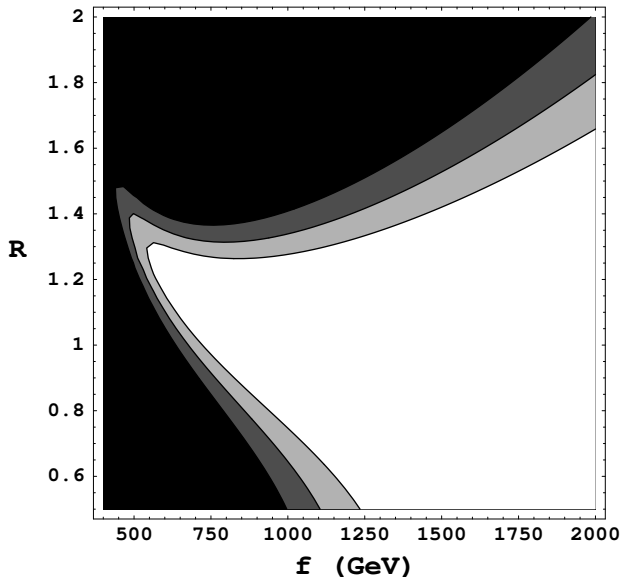


Figure 5: Exclusion contours in terms of the parameter $R = \lambda_1/\lambda_2$ and the symmetry breaking scale f . The contribution of the T-odd fermions to the T parameter is neglected. From lightest to darkest, the contours correspond to the 95, 99, and 99.9 confidence level exclusion.

With the assumption of flavor-diagonal and flavor-independent Yukawa couplings κ made in Section 3.2, the one-loop vertex corrections due to loops of T-odd fermions are flavor-universal, and can therefore be absorbed in the redefinitions of gauge couplings. They will not induce an observable shift in $Zb\bar{b}$ couplings.

4 Constraints on the Littlest Higgs Parameter Space

To obtain constraints on the parameter space of the LH model with T parity, we have performed a global fit to precision electroweak observables, including the LH contributions evaluated in the previous section. The LH contributions are parametrized by two dimensionless numbers, $R = \lambda_1/\lambda_2$ and δ_c , and the symmetry breaking scale f . In the fit, we have used the values of the 21 Z pole and low-energy observables listed in Ref. [17]; the equations expressing the shifts in these observables in terms of the oblique parameters and $\delta g_L^{b\bar{b}}$ are given in Ref. [21]. We take the top mass to be 176.9 GeV [17], and do not include the uncertainty associated with the top mass. In each constraint plot, we draw the 95, 99, and 99.9% confidence level contours in the context of a χ^2 analysis with two degrees of freedom⁶.

⁶It is important to note that changing the assumed number of degrees of freedom can strongly affect the positions of the contours; this is equivalent to modifying the priors that enter into the fit [22]. A complete Bayesian analysis taking into account a variety of different priors for the model parameters is

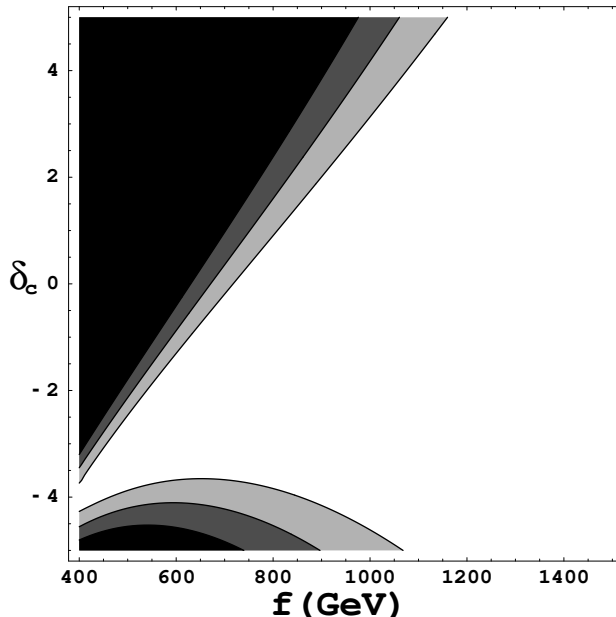


Figure 6: Exclusion contours in terms of the UV contribution to custodial symmetry violation δ_c , see Eq. (3.33), and f . From lightest to darkest, the contours correspond to the 95, 99, and 99.9 confidence level exclusion.

In the first part of the analysis, we have fixed the Higgs mass at its reference value, $m_{h,\text{ref}} = 113$ GeV. In Fig. 5, we plot the constraints in the $f - R$ plane, assuming $\delta_c = 0$. In Fig. 6, we fix $R = 1$ and plot the constraints in the $f - \delta_c$ plane, neglecting the T-odd fermion contribution. It is clear that a large part of the parameter space is consistent with precision electroweak constraints, including regions where the symmetry breaking scale f is as low as 500 GeV. (In these regions, a partial cancellation between the top and gauge sector contributions to the T parameter takes place.) In some cases, we have even obtained consistent fits for values of f as low as 350 GeV. However, since our analysis neglects all higher-derivative operators generated at the scale $\Lambda \sim 4\pi f$, which can contribute significantly to precision electroweak observables when $\Lambda \lesssim 5$ TeV, we estimate that the fits cannot be trusted for $f \lesssim 400$ GeV, and do not show that part of the parameter space in the plots.

As has been shown in Section 3.1, top sector loops in the LH model provide a sizable, positive contribution to the T parameter. This raises an interesting possibility: since the contribution of a heavy SM Higgs to the T parameter is negative, it is possible that these two effects partially cancel⁷, and a consistent fit is obtained for m_h far in excess of the usual

beyond the scope of this paper, but it would be straightforward to perform such an analysis using the formulas provided in Section 3.

⁷A consistent fit with a heavy Higgs can also be obtained in the Littlest Higgs model *without* T parity, where a positive correction to the T parameter is generated at tree level; however, this requires a rather high value of f , of order 5 TeV [22]. A similar cancellation of the heavy Higgs and new physics contributions

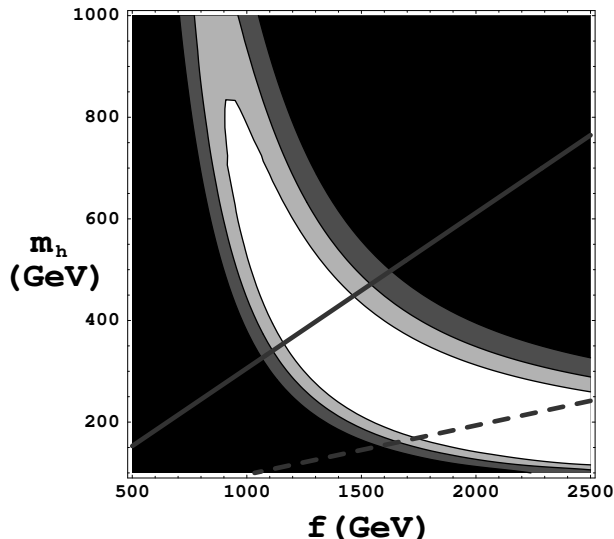


Figure 7: Exclusion contours in terms of the Higgs mass m_h and the symmetry breaking scale f . From lightest to darkest, the contours correspond to the 95, 99, and 99.9 confidence level exclusion. Contours of constant values of the fine-tuning parameter F are also shown; the solid and dashed lines correspond to $F = 10$ and $F = 100$, respectively.

SM upper bound, currently about 250 GeV. This possibility is illustrated in Fig. 7, where we fix $R = 2$, $\delta_c = 0$, and plot the constraints in the $f - m_h$ plane. Remarkably, values of m_h as high as 800 GeV are allowed at 95% confidence level. (Note that the approximation made in Eq. (3.35), where the corrections of order v/f in the Higgs contribution to the oblique parameters have been neglected, is justified in the region of interest, since f is still of order 1 TeV.) Thus, the LH model provides an explicit, well-motivated example of a theory in which the SM upper bound on the Higgs mass is avoided. Moreover, from the point of view of fine tuning in the Higgs potential, the high values of m_h are more natural in the context of this model [25]. For example, let us use the ratio of the one-loop top contribution to m_h^2 to the full m_h^2 ,

$$F = \frac{3\lambda_t^2 m_{T+}^2}{4\pi^2 m_h^2} \log \frac{\Lambda^2}{m_{T+}^2}, \quad (4.43)$$

as a quantitative measure of the fine tuning. (Larger values of F correspond to higher degree of fine tuning.) Plotting the contours of constant F indicates that, in the region of the parameter space consistent with precision electroweak constraints, the degree of fine tuning increases with the decreasing Higgs mass. Large values of m_h are clearly preferred from the point of view of naturalness in the Higgs potential.

If T parity is an exact symmetry (including the theory completing the description to T also occurs in top seesaw models [23]; see Ref. [24]. We are grateful to Bogdan Dobrescu for bringing this paper to our attention.

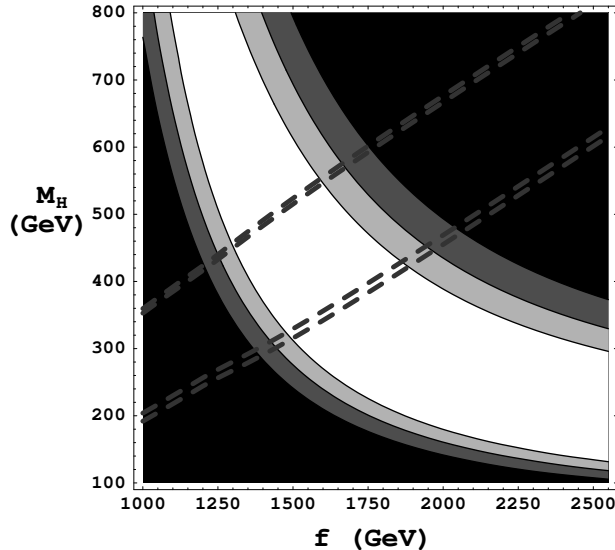


Figure 8: In this plot, the lines of constant relic density of the LTP are superimposed upon the constraints from the precision electroweak observables in the $f - m_h$ plane. In the narrow bands between the pairs of dashed lines, the LTP relic density is within 2σ of the central value provided by the WMAP collaboration [26]. For the detailed analysis of the LTP relic density, see Ref. [13].

above the scale Λ), the lightest T-odd particle (LTP) is stable. Generically, the LTP is the T-odd partner of the hypercharge gauge boson, which is electrically neutral and can play the role of WIMP dark matter. The LTP relic density has been computed in Ref. [13], and a region in the parameter space where the LTP can account for all of the observed dark matter has been identified. In Fig. 8, the 2 sigma contours on the dark matter relic density are superposed over a plot of the precision electroweak constraints where $R = 2$, $\delta_c = 0$, and m_h and f are allowed to vary. There is a region of the allowed parameter space in which the LTP can account for all of the dark matter.

In Figs. 5–8, the contribution of the T-odd fermions to the T parameter is neglected. This approximation is justified as long as the T-odd fermions are sufficiently light: for example, for T-odd fermion mass of 300 GeV, their total contribution to the T parameter is very small, and does not have any noticeable effect on the fits. On the other hand, heavier T-odd fermions can have a substantial effect. This is illustrated in Fig. 9, where the T-odd fermion contribution has been assumed to have the maximal size consistent with the constraint from four-fermi interactions, Eq. (3.41). (This corresponds to the T-odd fermion masses saturating the upper bound in Eq. (3.39).) While the constraints in this case are more severe, consistent fits can still be obtained for values of f below 1 TeV.

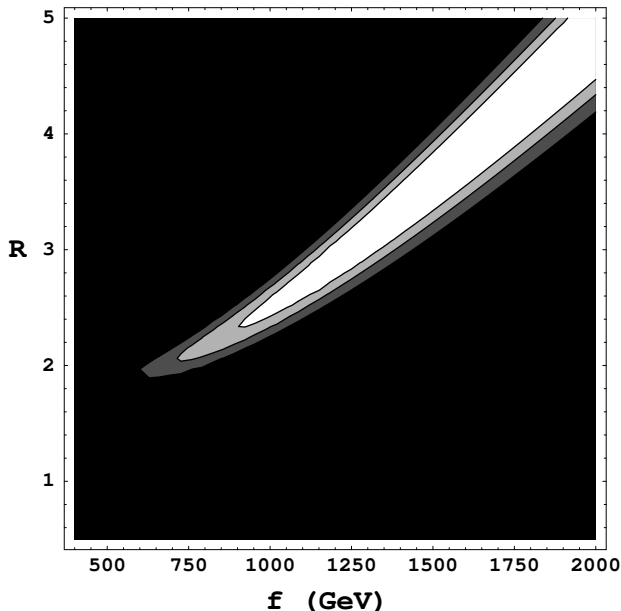


Figure 9: Exclusion contours in terms of the parameter $R = \lambda_1/\lambda_2$ and the symmetry breaking scale f . The contribution of the T-odd fermions to the T parameter is included assuming that it has the maximal size consistent with the constraint from four-fermi interactions, Eq. (3.41). From lightest to darkest, the contours correspond to the 95, 99, and 99.9 confidence level exclusion.

5 Conclusions

In this paper we have calculated the dominant corrections to the precision electroweak observables at the one-loop level in the Littlest Higgs model with T parity [11]. We performed a global fit to the precision electroweak observables and found that a large part of the model parameter space is consistent with data. In particular, a consistent fit can be obtained for values of the $SO(5)$ symmetry breaking scale f as low as 500 GeV. Furthermore, we found that the LH model can fit the data for values of the Higgs mass far in excess of the SM upper bound, due to the possibility of a partial cancellation between the contributions to the T parameter from Higgs loops and new physics. Combining our results with those of Ref. [13], we found that there are regions of parameter space allowed by precision electroweak constraints where the lightest T-odd particle can account for all of the observed dark matter.

We have argued that the corrections to low energy observables in the LH model are dominated by the top sector, and our analysis was primarily focused on those contributions. It would be interesting to perform a more detailed analysis of the effects from the gauge and scalar sectors; however, we do not expect these effects to substantially modify our conclusions. The analysis of the T-odd fermion sector in this paper relied on rather restrictive simplifying assumptions: in particular, the Yukawa couplings in the T-odd sector

were assumed to be flavor-diagonal and flavor-independent. A possible non-trivial flavor structure of their couplings could have interesting experimental consequences. Moreover, these fermions should be sufficiently light to be pair-produced at the LHC, or even at the Tevatron. It is therefore important to analyze that sector of the model in more detail.

In conclusion we find that the Littlest Higgs model with T parity is only weakly constrained by precision electroweak data, and provides a viable alternative for physics at the TeV scale. Apart from being theoretically attractive, the model has several features that are of interest for planning future experiments. Two examples are the possibility of a relatively heavy Higgs, as discussed in this paper, and the similarity of many of the collider signatures of this model to the benchmark SUSY signatures, which will inevitably complicate the LHC analysis [13]. We hope that our analysis, which explicitly demonstrates the viability of the LH model, will open the door for further detailed studies of its collider phenomenology.

Acknowledgements

We would like to thank Bogdan Dobrescu and Ian Low for useful discussions related to this work. We would also like to acknowledge helpful correspondence with Thomas Gregoire. This work is supported by the National Science Foundation under grant PHY-0355005.

A Renormalizable Gauges for the Littlest Higgs with T Parity

While the higher-order corrections for observable quantities in gauge theories must be gauge independent, an appropriate gauge choice can greatly reduce the complexity of a loop calculation, and make the underlying physics more transparent. This is especially important in the case of spontaneously broken gauge symmetries. While many issues in these theories are most easily understood in the unitary gauge, this gauge is ill-suited for loop calculations, leading to complicated intermediate expressions, and, in some cases, ambiguous answers⁸. Experience with the SM radiative correction calculations indicates that it is best to use the renormalizable, or R_ξ , gauges; a special case of $\xi = 1$, the 't Hooft-Feynman gauge, is especially useful. In this paper, we have used this gauge to calculate the $Zb\bar{b}$ coupling shift, see Section 3.3. Since only unitary-gauge Feynman rules have appeared in the literature so far for the LH models [28, 29], we will briefly discuss the R_ξ gauges for the LH model with T parity in this Appendix. We will focus on the charged gauge boson sector; the analysis of the neutral sector is similar. Even though the calculations in the

⁸A well-known example of such an ambiguity appears in the calculation of the W boson contribution to the anomalous magnetic moment of the muon [27].

paper do not require it, in this Appendix we will keep all correction of order $(v/f)^2$, since an interesting effect of $\omega - \phi$ mixing first appears at that order.

The charged gauge boson mass matrix follows from Eq. (2.4); to order ϵ^2 (where $\epsilon = v/f$) it has the form

$$M^2 = f^2 \begin{pmatrix} g_1^2 & -g_1 g_2 (1 - \epsilon^2/4) \\ -g_1 g_2 (1 - \epsilon^2/4) & g_2^2 \end{pmatrix}. \quad (\text{A.44})$$

Diagonalizing this matrix results in the mass eigenstates

$$W_L = c_0 W_1 + s_0 W_2, \quad W_H = -s_0 W_1 + c_0 W_2. \quad (\text{A.45})$$

In the LH model with T parity, the gauge couplings are set equal, $g_1 = g_2 = \sqrt{2}g$ and the mixing angle is given by $s_0 = c_0 = 1/\sqrt{2}$. The charged gauge boson mass eigenvalues are then

$$M_H^2 = g^2 f^2 \left[1 - \frac{1}{4} \epsilon^2 + \dots \right], \quad M_L^2 = \frac{g^2 v^2}{4} \left[1 - \frac{1}{6} \epsilon^2 + \dots \right]. \quad (\text{A.46})$$

Spontaneous breaking of the gauge symmetries leads to the kinetic mixing between the gauge bosons and the Goldstone boson fields in Eq. (2.7). In the mass eigenbasis, the mixing terms have the form

$$\begin{aligned} \mathcal{L}_{W\pi} = & M_H W_H^{\mu-} \left[\partial_\mu \omega^+ \left(1 - \frac{1}{24} \epsilon^2 \right) - \frac{i}{6} \epsilon^2 \partial_\mu \phi^+ \right] \\ & + M_L W_L^- \partial_\mu \pi^+ \left(1 - \frac{1}{12} \epsilon^2 \right) + \text{h.c.} \end{aligned} \quad (\text{A.47})$$

At order ϵ^2 , the Goldstone boson fields in Eq. (2.7) are not canonically normalized. To canonically normalize the Goldstone fields, we perform the following rescaling:

$$\begin{aligned} \pi^\pm & \rightarrow \pi^\pm \left(1 + \frac{1}{12} \epsilon^2 \right), \\ \omega^\pm & \rightarrow \omega^\pm \left(1 + \frac{1}{24} \epsilon^2 \right), \\ \phi^\pm & \rightarrow \phi^\pm \left(1 + \frac{1}{24} \epsilon^2 \right). \end{aligned} \quad (\text{A.48})$$

After this redefinition, there are still kinetic mixing terms involving the ω fields and the complex triplet, ϕ :

$$\mathcal{L}_{\text{kin}} = \partial_\mu \omega^+ \partial^\mu \omega^- + \partial_\mu \phi^+ \partial^\mu \phi^- + \frac{i}{12} \epsilon^2 (\partial_\mu \omega^+ \partial^\mu \phi^- - \partial_\mu \phi^+ \partial^\mu \omega^-). \quad (\text{A.49})$$

These terms are diagonalized with the redefinition

$$\begin{aligned} \omega'^\pm & = \omega^\pm \mp \frac{i}{24} \epsilon^2 \phi^\pm, \\ \phi'^\pm & = \phi^\pm \pm \frac{i}{24} \epsilon^2 \omega^\pm. \end{aligned} \quad (\text{A.50})$$

In terms of these new canonically normalized fields, the gauge boson-Goldstone mixing terms are given by⁹

$$\begin{aligned}\mathcal{L}_{W\pi} = & M_H W_H^{\mu-} \left[\partial_\mu \omega'^+ - \frac{i}{8} \epsilon^2 \partial_\mu \phi'^+ \right] \\ & + M_L W_L^- \partial_\mu \pi^+ + \text{h.c.}\end{aligned}\quad (\text{A.51})$$

A final rotation which leaves the kinetic terms diagonal,

$$\begin{aligned}\omega''^\pm &= \omega'^\pm \mp \frac{i}{8} \epsilon^2 \phi'^\pm, \\ \phi''^\pm &= \phi'^\pm \mp \frac{i}{8} \epsilon^2 \omega'^\pm,\end{aligned}\quad (\text{A.52})$$

identifies ω''^\pm as the combination of Goldstones eaten by the heavy gauge bosons, and ϕ''^\pm as the uneaten combination. A similar, but algebraically more involved, analysis carries through for the massive neutral gauge bosons.

Following the usual logic of renormalizable gauges, we add a gauge-fixing term which, after integration by parts, cancels the mixing terms:

$$\Delta\mathcal{L} = \frac{1}{2\xi_L} |\partial_\mu W_{L\mu}^\pm + M_L \xi_L \pi^\pm|^2 + \frac{1}{2\xi_H} |\partial_\mu W_H^\pm + M_H \xi_H \omega''^\pm|^2. \quad (\text{A.53})$$

The mass eigenstates in the eaten Goldstone sector are π^\pm , with mass $\sqrt{\xi_L} M_L$, and ω''^\pm , with mass $\sqrt{\xi_H} M_H$. (We have used the 't Hooft–Feynman gauge, $\xi_L = 1$, in Section 3.3.) Note that the π fields do not mix with ω and ϕ at any order in v/f , since such mixing is forbidden by T parity. The situation would be considerably more involved in the case of the Littlest Higgs without T parity.

Given the exact identification of the π^\pm fields in Eq. (2.7) with the lighter mass eigenstate in the R_ξ gauges, it is straightforward to obtain the $bt\pi$ and $bT\pi$ vertices required in the calculation of Section 3.3. Expanding the Σ matrices in Eq. (2.18) to linear order in Π , and using Eqs. (2.19), (2.21) to transform to the mass eigenbasis for the top sector, we obtain

$$-i\sqrt{2}\lambda_1 \bar{b}_{L+} \pi^- (\cos\alpha t_R + \sin\alpha T_{R+}) + \text{h.c.} = -i\lambda_t \bar{b}_{L+} \pi^- \left(t_R + \frac{\lambda_1}{\lambda_2} T_{R+} \right) + \text{h.c.} \quad (\text{A.54})$$

where λ_t is the SM Yukawa coupling, and b_+ is identified with the SM b quark. Note that the couplings involving the b_+ and any one of the T-odd Goldstone bosons, ϕ , ω or η , vanish due to the structure of the Lagrangian (2.18) and the fact that the field u_R is T-even.

⁹Note that the normalizations of the fields in the definition of the Goldstone boson matrix, Eq. (2.7), have been chosen so that the mixing term has the simple form in Eq. (A.51).

References

- [1] N. Arkani-Hamed, A. G. Cohen, E. Katz and A. E. Nelson, JHEP **0207**, 034 (2002) [arXiv:hep-ph/0206021].
- [2] For a recent review and a comprehensive collection of references, see M. Schmaltz and D. Tucker-Smith, arXiv:hep-ph/0502182.
- [3] C. Csaki, J. Hubisz, G. D. Kribs, P. Meade and J. Terning, Phys. Rev. D **67**, 115002 (2003) [arXiv:hep-ph/0211124]; Phys. Rev. D **68**, 035009 (2003) [arXiv:hep-ph/0303236].
- [4] J. L. Hewett, F. J. Petriello and T. G. Rizzo, JHEP **0310**, 062 (2003) [arXiv:hep-ph/0211218].
- [5] M. Perelstein, M. E. Peskin and A. Pierce, Phys. Rev. D **69**, 075002 (2004) [arXiv:hep-ph/0310039].
- [6] M. C. Chen and S. Dawson, Phys. Rev. D **70**, 015003 (2004) [arXiv:hep-ph/0311032].
- [7] D. E. Kaplan and M. Schmaltz, JHEP **0310**, 039 (2003) [arXiv:hep-ph/0302049]; M. Schmaltz, JHEP **0408**, 056 (2004) [arXiv:hep-ph/0407143].
- [8] S. Chang and J. G. Wacker, Phys. Rev. D **69**, 035002 (2004) [arXiv:hep-ph/0303001].
- [9] E. Katz, A. E. Nelson and D. G. E. Walker, arXiv:hep-ph/0504252.
- [10] H. C. Cheng and I. Low, JHEP **0309**, 051 (2003) [arXiv:hep-ph/0308199].
- [11] H. C. Cheng and I. Low, JHEP **0408**, 061 (2004) [arXiv:hep-ph/0405243].
- [12] I. Low, JHEP **0410**, 067 (2004) [arXiv:hep-ph/0409025].
- [13] J. Hubisz and P. Meade, Phys. Rev. D **71**, 035016 (2005) [arXiv:hep-ph/0411264].
- [14] C. F. Berger, M. Perelstein and F. Petriello, arXiv:hep-ph/0512053.
- [15] M. E. Peskin and T. Takeuchi, Phys. Rev. D **46**, 381 (1992).
- [16] A. Manohar and H. Georgi, Nucl. Phys. B **234**, 189 (1984); H. Georgi and L. Randall, Nucl. Phys. B **276**, 241 (1986).
- [17] S. Eidelman *et al.* [Particle Data Group], Phys. Lett. B **592**, 1 (2004).
- [18] J. Bernabeu, A. Pich and A. Santamaria, Phys. Lett. B **200**, 569 (1988).
- [19] M. S. Chanowitz, Phys. Rev. Lett. **87**, 231802 (2001) [arXiv:hep-ph/0104024].
- [20] P. Bamert, C. P. Burgess, J. M. Cline, D. London and E. Nardi, Phys. Rev. D **54**, 4275 (1996) [arXiv:hep-ph/9602438].

- [21] C. P. Burgess, S. Godfrey, H. Konig, D. London and I. Maksymyk, Phys. Rev. D **49**, 6115 (1994) [arXiv:hep-ph/9312291].
- [22] G. Marandella, C. Schappacher and A. Strumia, Nucl. Phys. B **715**, 173 (2005) [arXiv:hep-ph/0502095]; arXiv:hep-ph/0502096.
- [23] B. A. Dobrescu and C. T. Hill, Phys. Rev. Lett. **81**, 2634 (1998) [arXiv:hep-ph/9712319]; R. S. Chivukula, B. A. Dobrescu, H. Georgi and C. T. Hill, Phys. Rev. D **59**, 075003 (1999) [arXiv:hep-ph/9809470]; H. Collins, A. K. Grant and H. Georgi, Phys. Rev. D **61**, 055002 (2000) [arXiv:hep-ph/9908330].
- [24] R. S. Chivukula, C. Hoelbling and N. J. Evans, Phys. Rev. Lett. **85**, 511 (2000) [arXiv:hep-ph/0002022].
- [25] J. A. Casas, J. R. Espinosa and I. Hidalgo, JHEP **0503**, 038 (2005) [arXiv:hep-ph/0502066].
- [26] D. N. Spergel *et al.*, Astrophys. J. Suppl. **148**, 175 (2003) [astro-ph/0302209].
- [27] K. Fujikawa, B. W. Lee and A. I. Sanda, Phys. Rev. D **6**, 2923 (1972).
- [28] G. Burdman, M. Perelstein and A. Pierce, Phys. Rev. Lett. **90**, 241802 (2003) [Erratum-ibid. **92**, 049903 (2004)] [arXiv:hep-ph/0212228].
- [29] T. Han, H. E. Logan, B. McElrath and L. T. Wang, Phys. Rev. D **67**, 095004 (2003) [arXiv:hep-ph/0301040].